7492 *Biochemistry* **2009,** *48,* 7492–7501
DOI: 10.1021/bi900532w

BIOCHEMISTRY
including biophysical chemistry & molecular biology
Article

Polymerization Fidelity of a Replicative DNA Polymerase from the Hyperthermophilic Archaeon *Sulfolobus solfataricus* P2[†]

Likui Zhang,[‡,#,+] Jessica A. Brown,[‡,§,#] Sean A. Newmister,[‡] and Zucai Suo*[,‡,§,∥,⊥,@]

[‡]*Department of Biochemistry,* [§]*Ohio State Biochemistry Program,* [∥]*Ohio State Biophysics Program,* [⊥]*Molecular, Cellular and Developmental Biology Program, and* [@]*Comprehensive Cancer Center, The Ohio State University, Columbus, Ohio 43210*
[#] *These authors contributed equally to this work.* [+] *Present address: State Key Laboratory of Microbial Resources, Institute of Microbiology, Chinese Academy of Sciences, 3A Datun Rd., Beijing 100101, P. R. China.*

Received March 28, 2009; Revised Manuscript Received May 19, 2009

ABSTRACT: *Sulfolobus solfataricus* P2 is an aerobic crenarchaeon which grows optimally at 80 °C and pH 2−4. This organism encodes a B-family DNA polymerase, DNA polymerase B1 (PolB1), which faithfully replicates its genome of 3 million base pairs. Using pre-steady-state kinetic methods, we estimated the fidelity of PolB1 to be in the range of 10^{-6} to 10^{-8}, or one error per 10^6 to 10^8 nucleotide incorporations in vivo. To discern how the polymerase and 3′ → 5′ exonuclease activities contribute to the high fidelity of PolB1, an exonuclease-deficient mutant of PolB1 was constructed by mutating three conserved residues at the exonuclease active site. The base substitution fidelity of this mutant was kinetically measured to be in the range of 10^{-4} to 10^{-6} at 37 °C and pH 7.5. PolB1 exhibited high fidelity due to large differences in both ground-state nucleotide binding affinity and nucleotide incorporation rates between correct and incorrect nucleotides. The kinetic partitioning between the slow mismatch extension catalyzed by the polymerase activity and the fast mismatch excision catalyzed by the 3′ → 5′ exonuclease activity further lowers the error frequency of PolB1 by 14-fold. Furthermore, the base substitution error frequency of the exonuclease-deficient PolB1 increased by 5-fold as the reaction temperature increased. Interestingly, the fidelity of the exonuclease-deficient PolB1 mutant increased by 36-fold when the buffer pH was lowered from 8.5 to 6.0. A kinetic basis for these temperature and pH changes altering the fidelity of PolB1 was established. The faithful replication of genomic DNA catalyzed by PolB1 is discussed.

DNA polymerases are known to catalyze genomic replication, DNA damage repair, and DNA lesion bypass. Since the discovery of *Escherichia coli* DNA polymerase I in the 1950s, six families (A, B, C, D, X, and Y) of DNA polymerases have been discovered in all three domains of life (*1*, *2*). The B-family is mainly composed of eukaryotic replicative DNA polymerases, although some have been identified in archaea, bacteria, phages, and viruses (*2*). Among the B-family members, archaeal DNA polymerases have been studied as model enzymes in attempting to understand DNA replication in the more complicated eukaryotic systems. In addition to template-dependent polymerase activity, most B-family enzymes also possess 3′ → 5′ exonuclease activity which detects and removes errors catalyzed by the polymerase domain. Such an editing function enhances the fidelity of replicative DNA polymerases by ∼200-fold (*3*, *4*). The overall fidelity of numerous replicative DNA polymerases, estimated using either steady-state kinetics (*5*, *6*), pre-steady-state kinetics (*5*, *7*−*12*), or M13mp2-based forward and reversion mutation assays (*13*−*16*), is in the range of 10^{-6} to 10^{-8}, i.e., one error per 10^6 to 10^8 nucleotide incorporations. This high polymerization fidelity is essential for maintaining genomic stability from generation to generation (*17*).

Sulfolobus solfataricus is an aerobic crenarchaeon that metabolizes sulfur and grows optimally at 80 °C and pH 2−4 (*18*). The genome of *S. solfataricus* P2 has been completely sequenced and contains 2992245 base pairs (*18*). This hyperthermophile encodes only four DNA polymerases: three in the B-family (PolB1,[1] PolB2, and PolB3) and one in the Y-family (DNA polymerase IV, Dpo4). Among these four DNA polymerases, PolB2 and PolB3, which are identified on the basis of sequence homology,

[†]This work was supported by a National Science Foundation Career Award to Z.S. (Grant MCB-0447899). J.A.B. was supported by the National Institutes of Health Chemistry and Biology Interface Program at The Ohio State University (Grant 5 T32 GM008512-11).

*To whom correspondence should be addressed: 880 Biological Sciences, 484 W. 12th Ave., Columbus, OH 43210. Telephone: (614) 688-3706. Fax: (614) 292-6773. E-mail: suo.3@osu.edu.

[1]Abbreviations: BSA, bovine serum albumin; dNTP, 2′-deoxynucleoside 5′-triphosphate; Dpo4, *S. solfataricus* P2 DNA polymerase IV; DTT, dithiothreitol; EDTA, ethylenediaminetetraacetic acid; HIV-1 RT, human immunodeficiency virus type 1 reverse transcriptase; hPolγ, human mitochondrial DNA polymerase γ; PolB1, *S. solfataricus* DNA polymerase B1; PolB2, *S. solfataricus* DNA polymerase B2; PolB3, *S. solfataricus* DNA polymerase B3; PolB1 exo-, exonuclease-deficient DNA polymerase B1; rPolβ, rat DNA polymerase β; T7 DNA Pol, T7 DNA polymerase; *Taq*, *Thermus aquaticus*.

 Published on Web 05/20/2009

have not been shown to be active in vitro (*18*−*20*). In contrast, Dpo4 catalyzes DNA polymerization and bypasses a myriad of DNA lesions (*21*). Its polymerase active site is flexible and solvent accessible and can accommodate bulky DNA lesions (*22*−*24*). The polymerization fidelity of Dpo4 with undamaged DNA has been measured to be in the range of 10^{-3} to 10^{-4}, or one error per 10^3 to 10^4 nucleotide incorporations, by utilizing both kinetic and M13mp2-based fidelity assays (*21*, *25*, *26*). PolB1, a replicative DNA polymerase (*27*−*29*), has been reported to possess both DNA polymerase and 3′ → 5′ exonuclease activities in vitro (*29*). The crystal structure of apo PolB1 shows that this enzyme, like A- and B-family DNA polymerases, contains an N-terminal proofreading 3′ → 5′ exonuclease domain and a C-terminal "right-hand" DNA polymerase domain (*30*). Thus, the polymerization fidelity of PolB1 is expected to be high but has not been reported. In this paper, we employed pre-steady-state kinetic methods to determine the base substitution fidelity and mismatch extension fidelity of PolB1. The effect of reaction temperature and pH on the polymerase selectivity and the contribution of the 3′ → 5′ exonuclease activity to the polymerization fidelity of PolB1 were also investigated.

EXPERIMENTAL PROCEDURES

Materials. Materials were purchased from the following companies: [γ-^{32}P]ATP, PerkinElmer (Boston, MA); dNTPs, GE Healthcare (Piscataway, NJ); Biospin columns, Bio-Rad Laboratories (Herclues, CA); OptiKinase, USB (Cleveland, OH); Quikchange XL site-directed mutagenesis kit, Stratagene (La Jolla, CA); and Wizard Plus SV Miniprep kit, Promega (Madison, WI).

Mutagenesis, Overexpression, and Purification of Wild-Type PolB1 and the Exonuclease-Deficient Mutant. The plasmid pET33b-PolB1, a generous gift from Dr. Hong Ling at the University of Western Ontario (London, ON), encodes *S. solfataricus* P2 PolB1 fused to a His_6 tag at the C-terminus. Two rounds of site-directed mutagenesis were performed to generate the exonuclease-deficient triple-point mutant (D231A, E233A, and D318A). First, a double mutant (D231A/E233A) was constructed using the wild-type PolB1 plasmid as a template. Then, the resulting plasmid was used to introduce the D318A mutation. The DNA sequence of the mutant plasmids was confirmed by sequencing (OSU Plant Microbe Genomics Facility).

Wild-type plasmid pET33b-PolB1 was transformed into *E. coli* expression strain BL21(DE3) Rosetta cells. An overnight culture of the Rosetta cells carrying the wild-type PolB1 plasmid was used to inoculate Luria-Bertani medium containing 50 μg/mL kanamycin and 25 μg/mL chloramphenicol. Cells were grown at 37 °C. Once the OD_{600} of the cells reached 0.6, cultures were induced with 0.15 mM IPTG and incubated at 30 °C until the OD_{600} reached 1.7. Induced cells were harvested and resuspended in buffer A [10 mM KH_2PO_4 (pH 7.0), 50 mM NaCl, 10 mM $MgCl_2$, 10% glycerol, 0.1% 2-mercaptoethanol, and 1 mM imidazole]. A protease inhibitor cocktail tablet (Roche) and PMSF (1 mM) were added to the cell paste. The cells were then lysed by being passed through a French press cell three times at 16000 psi. The cell lysate was clarified by ultracentrifugation (35000 rpm for 40 min). Clear lysate was subjected to heat denaturation at 74 °C for 14 min to precipitate thermolabile *E. coli* proteins which were subsequently removed by ultracentrifugation. The supernatant was incubated with IMAC Fastflow6 Ni^{2+}-charged resin (GE Healthcare) for 3 h in the presence of 10 mM imidazole, and the PolB1-bound resin was packed into a column. After being washed with buffer B [10 mM KH_2PO_4 (pH 7.0), 350 mM NaCl, 35 mM imidazole, 10% glycerol, and 0.05% 2-mercaptoethanol], PolB1 was eluted using a linear gradient from 35 to 500 mM imidazole in buffer B. Fractions containing PolB1 were pooled and then dialyzed against buffer C [50 mM Tris-HCl (pH 7.5 at 25 °C), 50 mM NaCl, 1 mM EDTA, 10% glycerol, and 0.1% 2-mercaptoethanol]. The dialyzed protein solution was passed through a HiTrap Q anion exchange column (GE Healthcare). The loading elute was applied to a HiTrap SP cation exchange column (GE Healthcare). The column-bound PolB1 was eluted using a gradient from 100 to 1000 mM NaCl in buffer C. The fractions containing PolB1 were pooled and dialyzed against buffer D [25 mM HEPES (pH 7.0 at 4 °C), 150 mM NaCl, 1 mM EDTA, 1 mM DTT, and 50% glycerol]. The dialyzed protein solution was then concentrated and stored at −80 °C. The apparent homogeneity of purified PolB1 (>95%) was assessed on the basis of Coomassie Blue-stained SDS−PAGE gels. The concentration of purified wild-type PolB1 was measured spectrophotometrically at 280 nm using the calculated extinction coefficient of 124785 M^{-1} cm^{-1}. Similarly, the exonuclease-deficient triple point mutant (D231A/E233A/D318A) of PolB1 was overexpressed, purified, and quantitated.

DNA Substrates. The synthetic oligonucleotides listed in Table 1 were purchased from Integrated DNA Technologies, Inc. (Coralville, IA), and purified as described previously (*26*). The primer strand 21-mer was 5′-radiolabeled with [γ-^{32}P]ATP and Optikinase and was annealed to the appropriate 41-mer (Table 1) as described previously (*26*).

Reaction Buffers. All experiments, if not specified, were performed in buffer A which contains 50 mM HEPES (pH 7.5 at all temperatures), 15 mM $MgCl_2$, 75 mM NaCl, 5 mM DTT, 10% glycerol, and 0.1 mg/mL BSA. Reactions were conducted at temperatures ranging from 19 to 50 °C either using a rapid chemical-quench flow apparatus (KinTek) or via manual quench. For buffer optimization and pH-dependent fidelity studies at 37 °C, assays were conducted in 25 mM MES buffer for pH values between 6.0 and 7.0, 50 mM HEPES at pH 7.5, 25 mM Tris-HCl at pH 8.0 and 8.5, and 25 mM glycine at pH 9.0 and 10.0. For both DNA polymerization and excision experiments, the enzyme·DNA complex was not pre-equilibrated in the presence of $MgCl_2$.

Polymerase and Exonuclease Single-Turnover Assays. For polymerization reaction assays, PolB1 (120 nM) was pre-incubated with D-DNA (30 nM) in buffer A before the reaction was initiated with varying concentrations of a single dNTP·Mg^{2+} (1−2400 μM). For DNA excision assays, PolB1 (400 nM) was pre-equilibrated with DNA (100 nM), and the reaction was initiated with the addition of Mg^{2+} (15 mM) in buffer A.

Product Analysis. Reaction products were analyzed by sequencing gel electrophoresis (17% acrylamide, 8 M urea, and 1× TBE running buffer) and quantitated using a Typhoon TRIO (GE Healthcare) and ImageQuant (Molecular Dynamics).

Data Analysis. All kinetic data were fit by nonlinear regression using KaleidaGraph (Synergy Software). Data from single-nucleotide incorporation experiments under single-turnover conditions were fit to eq 1

$$[\text{product}] = A[1 - \exp(-k_{obs}t)] \quad (1)$$

Table 1: Sequences of Synthetic Double-Stranded DNA Substrates

D-1	5′-CGCAGCCGTCCAACCAACTCA-3′ 3′-GCGTCGGCAGGTTGGTTGAGTAGCAGCTAGGTTACGGCAGG-5′
D-6	5′-CGCAGCCGTCCAACCAACTCA-3′ 3′-GCGTCGGCAGGTTGGTTGAGTGGCAGCTAGGTTACGGCAGG-5′
D-7	5′-CGCAGCCGTCCAACCAACTCA-3′ 3′-GCGTCGGCAGGTTGGTTGAGTTGCAGCTAGGTTACGGCAGG-5′
D-8	5′-CGCAGCCGTCCAACCAACTCA-3′ 3′-GCGTCGGCAGGTTGGTTGAGTCGCAGCTAGGTTACGGCAGG-5′
M-1	5′-CGCAGCCGTCCAACCAACTCAA-3′ 3′-GCGTCGGCAGGTTGGTTGAGTAGCAGCTAGGTTACGGCAGG-5′

where A and k_{obs} represent the reaction amplitude and observed rate, respectively. Data from the plot of k_{obs} versus nucleotide concentrations were fit to eq 2

$$k_{obs} = k_p[\text{dNTP}]/(K_d + [\text{dNTP}]) \quad (2)$$

where k_p is the maximum rate of nucleotide incorporation and K_d is the equilibrium dissociation constant of a dNTP. When K_d is too large, the plot of k_{obs} versus nucleotide concentration was fit to eq 3

$$k_{obs} = (k_p/K_d)[\text{dNTP}] \quad (3)$$

which extracted the substrate specificity constant, k_p/K_d.

Data from DNA excision experiments under single-turnover conditions were fit to eq 4

$$[\text{product}] = A \exp(-k_{exo}t) \quad (4)$$

where A and k_{exo} represent the reaction amplitude and observed DNA excision rate, respectively.

RESULTS

Generation of the 3′ → 5′ Exonuclease-Deficient Mutant of PolB1. It has been demonstrated previously that PolB1 (882 amino acid residues and 101.2 kDa) from *S. solfataricus* P2 possesses a strong 3′ → 5′ exonuclease activity (*29*), which would complicate the interpretation of the kinetic data of nucleotide incorporation. To eliminate this problem, we constructed an exonuclease-deficient mutant of PolB1 (PolB1 exo-) by substituting an alanine for conserved residues D231, E233, and D318, which are located in the conserved sequence motifs Exo I and II among the B-family DNA polymerases (*27*). On the basis of X-ray crystal structural analysis (*30*) and primary sequence alignment (*27*), these three residues and D413 bind two Mg^{2+} ions required for catalysis. Following the successful site-directed mutagenesis and purification processes, we examined the activity of both the polymerase and exonuclease functions. A pre-incubated solution of PolB1 (wild-type or exo-) and 5′-^{32}P-labeled D-1 DNA (Table 1) was mixed with either 50 μM dTTP·Mg^{2+}, 50 μM dCTP·Mg^{2+}, or Mg^{2+}. Our data confirmed that wild-type PolB1 exhibited efficient exonuclease activity, for significant product degradation (<21-mer) was observed under all three reaction conditions (Figure 1A of the Supporting Information). In contrast, elongated DNA products accumulated for PolB1 exo- in the presence of both correct (dTTP) and incorrect (dCTP) nucleotides (Figure 1B of the Supporting Information). Furthermore, in the absence of nucleotides, only substrate (21-mer) was present for PolB1 exo- for reaction times from 15 s to 3 h (data not shown). Together, these results showed that PolB1 exo- lacked 3′ → 5′ exonuclease activity and its polymerase activity remained intact. Additionally, if one or two of the three residues (D231, E233, and D318) were mutated to alanine, the 3′ → 5′ exonuclease activity of the mutants decreased but was not completely eliminated (data not shown).

Optimization of the Reaction Conditions for the Polymerase Activity of PolB1. To optimize the reaction conditions for the polymerase activity of PolB1, all reaction components were kept constant while the concentrations of Mg^{2+} and NaCl and the buffer pH were individually altered. A pre-incubated solution of 120 nM PolB1 exo- and 30 nM 5′-[^{32}P]D-1 (Table 1) reacted with 100 μM dTTP·Mg^{2+} at 37 °C for various times before the reaction was quenched with 0.37 M EDTA. The time dependence of product concentration was fit to eq 1 (Experimental Procedures) to obtain the observed reaction rate, k_{obs}, and reaction amplitude (data not shown). Figure 1 shows that the k_{obs} values varied depending on the concentrations of Mg^{2+} and NaCl and with buffer pH. In comparison, the reaction amplitude was close to 30 nM under all conditions except at 70 mM Mg^{2+}, 250 mM NaCl, and pH 10. On the basis of the k_{obs} values and reaction amplitudes for single correct nucleotide incorporation, we concluded that the optimal reaction conditions for PolB1 exo- were 15 mM $MgCl_2$ (Figure 1A), 75 mM NaCl (Figure 1B), and pH 7.5 (Figure 1C). Under non-optimum conditions, dTTP incorporation occurred at significantly lower k_{obs} values. Therefore, all kinetic assays presented herein, if not specified, were performed in the optimized buffer A which contains 50 mM HEPES (pH 7.5 at 37 °C), 15 mM $MgCl_2$, 75 mM NaCl, 5 mM DTT, 10% glycerol, and 0.1 mg/mL BSA. Please note that most of the assays shown in this work and our accompanying paper (*31*) were performed at 37 °C, rather than 80 °C which is the in vivo temperature for PolB1. The reaction temperature of 37 °C was selected because (i) the rapid chemical-quench apparatus can function properly, (ii) the rates of correct nucleo-

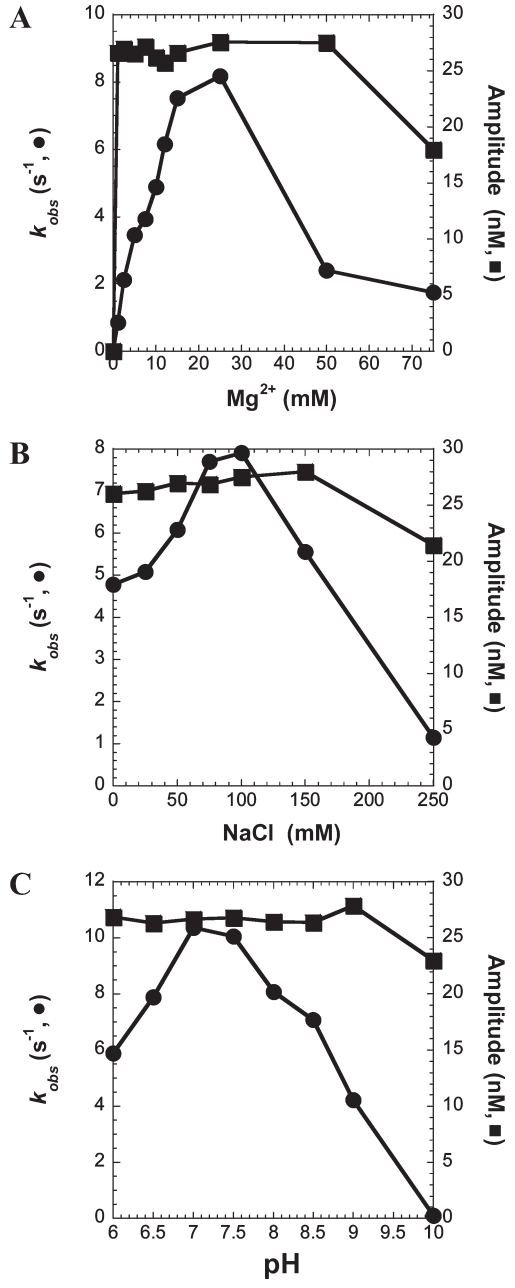

FIGURE 1: Effect of Mg^{2+} concentration, NaCl concentration, and pH on the enzymatic activity of PolB1 exo-. A pre-incubated solution of D-1 5′-labeled with ^{32}P (30 nM) and a 3-fold excess of PolB1 exo- (120 nM) was rapidly mixed with the correct nucleotide (100 μM dTTP) for various time intervals under single-turnover conditions. Each plot shows the k_{obs} values (●) and reaction amplitudes (■) as the (A) Mg^{2+} concentration, (B) NaCl concentration, or (C) buffer pH was varied. Activity in panel C was assayed in 25 mM MES-NaOH buffer between pH 6.0 and 7.0, in 25 mM Tris-HCl buffer for pH 8.0 and 8.5, and in 25 mM glycine-NaOH buffer for pH 9.0 and 10.0.

tide incorporation are within the range that can be accurately measured by the rapid chemical-quench apparatus, (iii) most of the DNA substrate 21/41-mer exists as a duplex, rather than single-stranded oligomers, during polymerization, and (iv) our fidelity and mechanism studies of Dpo4 revealed similar findings at both 37 and 56 °C (*26*, *32*, *33*).

Substrate Specificity and Base Substitution Fidelity of PolB1 exo- at 37 °C. It was expected that PolB1, like other replicative DNA polymerases, incorporates correct nucleotides with much higher substrate specificity than it incorporates

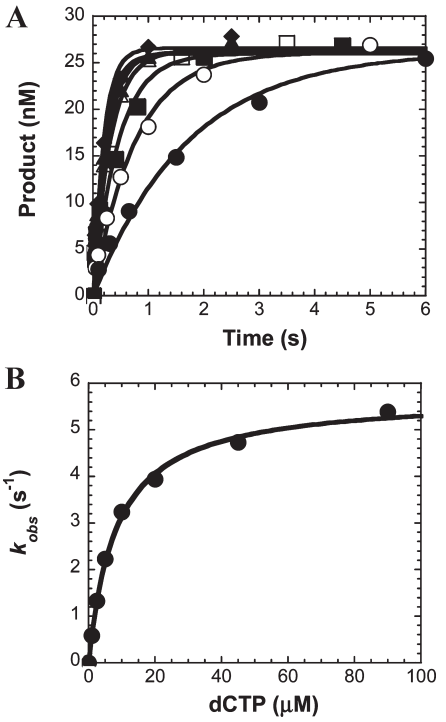

FIGURE 2: Dependence of concentration on the pre-steady-state rate of correct and incorrect nucleotide incorporation catalyzed by PolB1 exo-. (A) A pre-incubated solution of PolB1 exo- (120 nM) and 5′-^{32}P-labeled D-6 (30 nM) was mixed with various concentrations of dCTP·Mg^{2+} [1 (●), 2.5 (○), 5 (■), 10 (□), 20 (▲), 45 (△), and 90 μM (◆)] for various time intervals. The solid lines are the best fits to the single-exponential equation. (B) The single-turnover rates (k_{obs}) were plotted as a function of dCTP concentration. These data were then fit to a hyperbolic equation to yield a k_p of 5.7 ± 0.1 s^{-1} and a K_d of 8.2 ± 0.5 μM.

incorrect nucleotides. To determine the substrate specificity constant (k_p/K_d) of an incoming nucleotide, we measured the maximum incorporation rate constant (k_p) and the apparent equilibrium dissociation constant (K_d) of an incoming nucleotide (*34*). These two pre-steady-state kinetic parameters can be determined through the nucleotide concentration dependence of the observed incorporation rate (k_{obs}). Figure 2 is a representative example of these kinetic measurements determined under single-turnover reaction conditions, whereby the concentration of the enzyme was 4-fold greater than the DNA concentration to ensure that almost all of the DNA molecules were bound by PolB1 exo-. In Figure 2A, a pre-incubated solution of 120 nM PolB1 exo- and 30 nM 5′-^{32}P-labeled D-6 (Table 1) reacted with increasing concentrations of correct dCTP·Mg^{2+} in buffer A for various amounts of time prior to the reaction being quenched with 0.37 M EDTA. At each dCTP concentration, the product concentration was plotted as a function of the reaction time, and the data were fit to eq 1 (Experimental Procedures) to yield a k_{obs} (Figure 2A). In Figure 2B, the extracted k_{obs} values were plotted versus the corresponding dCTP concentration, and the data were subsequently fit to eq 2 (Experimental Procedures) to yield a k_p of 5.7 ± 0.1 s^{-1} and a K_d of 8.2 ± 0.5 μM for dCTP incorporation. The substrate specificity constant for incorporation of dCTP into D-6 was then calculated to be 0.70 μM^{-1} s^{-1}. Similarly, we measured the k_p, K_d, and k_p/K_d of the 15 other possible incorporations of a single nucleotide (correct and incorrect) into the four DNA substrates in Table 1 (data not shown), and the kinetic parameters are listed in Table 2. For several incorrect nucleotides, we could not determine the individual k_p and K_d

Table 2: Kinetic Parameters of Nucleotide Incorporation into DNA Catalyzed by PolB1 exo- at 37 °C

dNTP	k_p (s^{-1})	K_d (μM)	k_p/K_d (μM^{-1} s^{-1})	F_{pol}[a]
		Template dA (D-1)		
dTTP	8.2 ± 0.6	11 ± 2	7.5×10^{-1}	
dATP	1.3 ± 0.1	(2.8 ± 0.3) × 10^3	4.6×10^{-4}	6.2×10^{-4}
dCTP	–	–	1.9×10^{-4}	2.5×10^{-4}
dGTP	0.05 ± 0.01	(1.2 ± 0.2) × 10^3	4.2×10^{-5}	5.6×10^{-5}
		Template dT (D-7)		
dATP	11.5 ± 0.2	4.9 ± 0.3	2.3	
dCTP	0.7 ± 0.2	(3.3 ± 1.5) × 10^3	2.1×10^{-4}	9.0×10^{-5}
dGTP	0.9 ± 0.1	(3.2 ± 0.8) × 10^3	2.8×10^{-4}	1.2×10^{-4}
dTTP	1.7 ± 0.3	(4.5 ± 1.0) × 10^3	3.8×10^{-4}	1.6×10^{-4}
		Template dG (D-6)		
dCTP	5.7 ± 0.1	8.2 ± 0.5	7.0×10^{-1}	
dATP	–	–	7.5×10^{-6}	1.1×10^{-5}
dGTP	0.032 ± 0.002	(0.9 ± 0.1) × 10^3	3.3×10^{-5}	4.8×10^{-5}
dTTP	1.3 ± 0.2	(3.5 ± 0.7) × 10^3	3.7×10^{-4}	5.3×10^{-4}
		Template dC (D-8)		
dGTP	5.3 ± 0.1	4.1 ± 0.3	1.3	
dATP	0.34 ± 0.05	(2.3 ± 0.6) × 10^3	1.3×10^{-4}	1.0×10^{-4}
dCTP	0.009 ± 0.002	(2.0 ± 0.9) × 10^3	4.5×10^{-6}	3.5×10^{-6}
dTTP	–	–	1.6×10^{-4}	1.2×10^{-4}

[a] Calculated as $(k_p/K_d)_{incorrect}/[(k_p/K_d)_{correct} + (k_p/K_d)_{incorrect}]$.

values because of their extremely weak apparent ground-state binding affinity ($1/K_d$) for an incoming dNTP. Instead, we determined the k_p/K_d values by fitting the plots of k_{obs} versus nucleotide concentration to eq 3 in Experimental Procedures (data not shown). On average, incorrect nucleotides had ~370-fold weaker apparent ground-state binding affinities and were incorporated with 11-fold slower k_p values than correct nucleotides. The calculated substrate specificity constants indicated that correct nucleotides were incorporated with 10^3- to 10^5-fold higher efficiency than incorrect nucleotides. In addition, we calculated the base substitution fidelity of PolB1 exo- to be in the range of 10^{-4} to 10^{-6} (Table 2), or one mistake per 10^4 to 10^6 nucleotide incorporations at 37 °C.

Effect of Temperature on the Base Substitution Fidelity of PolB1 exo- at pH 7.5. Since *S. solfataricus* P2 grows optimally at 80 °C (*18*), it is important to kinetically determine the fidelity of PolB1 at its physiological temperature. However, this cannot be accomplished here because the rapid chemical-quench apparatus cannot be operated at 80 °C, and correct nucleotide incorporations catalyzed by PolB1 exo- at such a high temperature are predicted to be finished within the mixing dead time (1−3 ms) of the apparatus. To estimate the fidelity of PolB1 at 80 °C, we decided to determine the temperature dependence of the fidelity. Under single-turnover conditions, PolB1 exo- (120 nM) and 30 nM 5′-[^{32}P]D-1 (Table 1) were first pre-incubated on ice and then equilibrated at 19, 26, 32, 44, or 50 °C. Such a gradual increase in the incubation temperature helped to stabilize the DNA duplex at the polymerase active site of PolB1 exo-, especially at temperatures exceeding 37 °C. The pre-incubated solutions of D-1 and PolB1 were then reacted with increasing concentrations of correct dTTP·Mg^{2+} or incorrect dATP·Mg^{2+} for various times at the appropriate temperature. The reactions were quenched and analyzed as described above.

Table 3: Temperature Dependence of the Nucleotide Incorporation Fidelity Catalyzed by PolB1 exo-

dNTP	k_p (s^{-1})	K_d (μM)	k_p/K_d (μM^{-1} s^{-1})	F_{pol}[a]
		19 °C		
dTTP	0.14 ± 0.01	38 ± 6	3.7×10^{-3}	
dATP	0.0033 ± 0.0008	(4.0 ± 1.3) × 10^3	8.3×10^{-7}	2.2×10^{-4}
		26 °C		
dTTP	1.6 ± 0.01	18 ± 0.4	8.9×10^{-2}	
dATP	0.018 ± 0.008	(2.5 ± 1.5) × 10^3	7.2×10^{-5}	8.1×10^{-4}
		32 °C		
dTTP	2.6 ± 0.1	6.9 ± 0.5	3.8×10^{-1}	
dATP	0.19 ± 0.06	(2.3 ± 0.8) × 10^3	8.3×10^{-5}	2.2×10^{-4}
		37 °C		
dTTP	8.2 ± 0.6	11 ± 2	7.5×10^{-1}	
dATP	1.3 ± 0.1	(2.8 ± 0.3) × 10^3	4.6×10^{-4}	6.1×10^{-4}
		44 °C		
dTTP	38 ± 1	13 ± 1	2.9	
dATP	5.4 ± 1.3	(2.5 ± 0.8) × 10^3	2.2×10^{-3}	7.6×10^{-4}
		50 °C		
dTTP	92 ± 2	20 ± 1	4.6	
dATP	22 ± 5	(4.2 ± 1.5) × 10^3	5.2×10^{-3}	1.1×10^{-3}

[a] Calculated as $(k_p/K_d)_{incorrect}/[(k_p/K_d)_{correct} + (k_p/K_d)_{incorrect}]$.

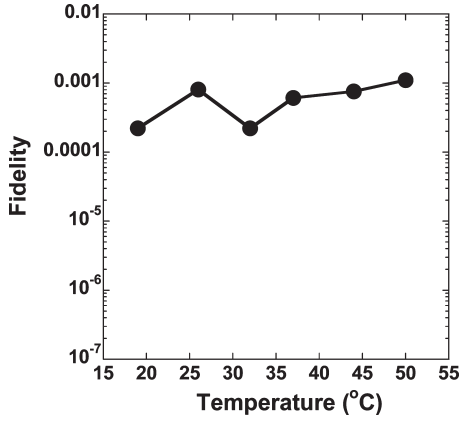

FIGURE 3: Temperature dependence of the nucleotide incorporation fidelity of PolB1 exo-.

The kinetic parameters for the incorporations of correct dTTP and incorrect dATP into D-1 are listed in Table 3. The k_p for both dTTP and dATP increased dramatically with reaction temperature while the apparent K_d changed slightly. Interestingly, the k_p/K_d for both correct and incorrect nucleotide incorporations increased with a similar magnitude at each temperature, leading to a modest change of 5-fold in the base substitution fidelity of PolB1 exo- from 19 to 50 °C (Figure 3).

Effect of pH on the Base Substitution Fidelity of PolB1 exo- at 37 °C. Although *S. solfataricus* P2 grows optimally at pH 2−4 (*18*), its cytoplasmic pH, which is unknown at present, is expected to be near neutral so that genomic stability is maintained. Because the cytoplasmic pH of *S. solfataricus* P2 may not be 7.5 as in our optimized reaction buffer, it is important to determine the effect of pH on the polymerase fidelity of PolB1.

Table 4: pH Dependence of the Nucleotide Incorporation Fidelity of PolB1 exo- at 37 °C

dNTP	k_p (s^{-1})	K_d (μM)	k_p/K_d (μM^{-1} s^{-1})	F_{pol}[a]
		pH 6.0		
dTTP	8.9 ± 0.3	3.2 ± 0.4	2.8	
dATP	0.19 ± 0.01	(2.9 ± 0.2) × 10^3	6.6 × 10^{-5}	2.4 × 10^{-5}
		pH 6.5		
dTTP	8.5 ± 0.2	4.5 ± 0.3	1.9	
dATP	0.32 ± 0.02	(2.2 ± 0.2) × 10^3	1.5 × 10^{-4}	7.9 × 10^{-5}
		pH 7.5		
dTTP	8.2 ± 0.6	11 ± 2	7.5 × 10^{-1}	
dATP	1.3 ± 0.1	(2.8 ± 0.3) × 10^3	4.6 × 10^{-4}	6.1 × 10^{-4}
		pH 8.5		
dTTP	5.8 ± 0.1	21 ± 0.4	2.8 × 10^{-1}	
dATP	2.0 ± 0.5	(8.4 ± 2.3) × 10^3	2.4 × 10^{-4}	8.6 × 10^{-4}

[a] Calculated as $(k_p/K_d)_{incorrect}/[(k_p/K_d)_{correct} + (k_p/K_d)_{incorrect}]$.

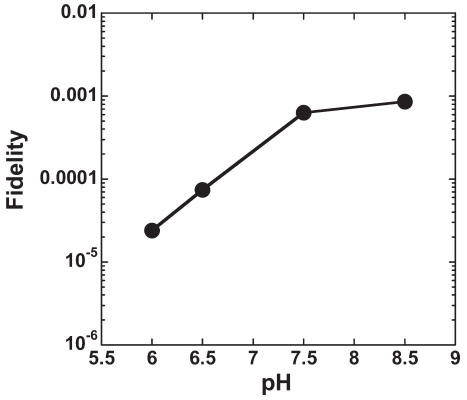

FIGURE 4: pH dependence of the nucleotide incorporation fidelity of PolB1 exo-.

Using similar kinetic assays described above, we measured the kinetic parameters (Table 4) for the incorporations of correct dTTP and incorrect dATP into D-1 (Table 1) at 37 °C catalyzed by PolB1 exo- at different buffer pH values (6.0, 6.5, and 8.5). For dTTP incorporation, the k_p (from 5.8 to 8.9 s^{-1}) changed insignificantly while the apparent K_d increased from 3.2 to 21 μM when the buffer pH changed from 6.0 to 8.5. In contrast, the k_p for the incorrect dATP incorporation changed significantly from 0.19 to 2.0 s^{-1} with an increase in buffer pH from 6.0 to 8.5. However, the pH did not affect the apparent K_d of dATP until the pH was 8.5, whereby a 6-fold increase was observed from pH 6.5 to 8.5. Interestingly, when the buffer pH changed from 6.0 to 8.5, the calculated substrate specificity constant for correct dTTP incorporation decreased by ~10-fold while the k_p/K_d for dATP misincorporation increased by ~4-fold, leading to a 36-fold decrease in the base substitution fidelity of PolB1 exo- (Table 4 and Figure 4). Thus, PolB1 exo- had higher polymerase efficiency and fidelity at a relatively low pH.

Mismatch Extension Fidelity of PolB1 exo- at 37 °C. When PolB1 exo- misincorporates a nucleotide, it may continue polymerization to bury the misincoporation by either a correct or incorrect nucleotide. Under similar single-turnover conditions as described above, we measured the kinetic parameters (Table 5) for each of the four possible incorporations into M-1 which

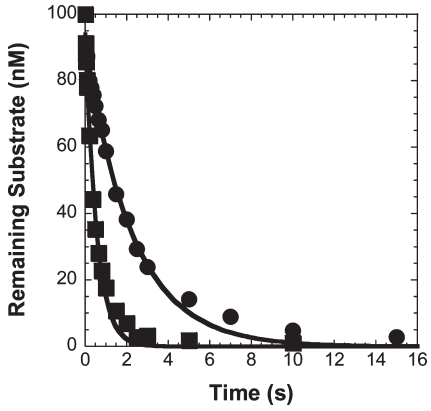

FIGURE 5: Rate of 3′ → 5′ exonuclease activity catalyzed by PolB1. A pre-incubated solution of PolB1 (400 nM) and DNA (100 nM) was rapidly mixed with Mg^{2+} (15 mM) for various reaction times. The amount of remaining substrate was plotted as a function of time. The solid lines represent the best fit to a single-exponential decay. PolB1 catalyzed the excision of a nucleotide for a matched [D-1 DNA (●)] or mismatched [M-1 DNA (■)] DNA terminus at rates of 0.44 ± 0.02 and 1.86 ± 0.08 s^{-1}, respectively.

Table 5: Fidelity of the Extension of a Mismatched dA·dA Terminus Catalyzed by PolB1 exo- at 37 °C

dNTP	k_p (s^{-1})	K_d (μM)	k_p/K_d (μM^{-1} s^{-1})	F_{ext}[a]
dCTP	0.13 ± 0.01	(1.0 ± 0.2) × 10^3	1.3 × 10^{-4}	
dATP		no observed incorporation		
dGTP		no observed incorporation		
dTTP	–	–	3.8 × 10^{-7}	2.9 × 10^{-3}

[a] Calculated as $(k_p/K_d)_{incorrect}/[(k_p/K_d)_{correct} + (k_p/K_d)_{incorrect}]$.

contains a mismatched dA·dA base pair at its primer−template junction (Table 1). Among the four nucleotides, the correct dCTP was incorporated by PolB1 exo- with the highest substrate specificity constant (Table 5). Notably, the k_p, apparent K_d, and k_p/K_d values of dCTP are comparable to the corresponding values of several misincorporations in Table 2, e.g., incorrect dATP into D-8. While the incorporations of incorrect nucleotides dATP and dGTP were not observed even after 3 h (data not shown), misincorporation of dTTP into M-1 was readily detected, and the substrate specificity constant was determined to be 3.8 × 10^{-7} (Table 5). However, the k_p and apparent K_d values for dTTP misincorporation were not determined due to an extremely weak apparent ground-state binding affinity (see above). On the basis of the substrate specificity constants, the extension fidelity was calculated to be 2.9 × 10^{-3} for dTTP or higher for dATP and dGTP (Table 5).

Exonuclease Cleavage of Double-Stranded DNA Substrates Containing Matched and Mismatched 3′-Terminal Nucleotides at 37 °C. The 3′ → 5′ exonuclease activity of a replicative DNA polymerase is known to proofread polymerization products and excise misincorporated nucleotides. To examine if the 3′ → 5′ exonuclease activity of PolB1 has a similar function, we measured the excision rate (k_{exo}) of wild-type PolB1 with both D-1 and M-1 (Table 1) under single-turnover conditions. Wild-type PolB1 (400 nM) and 5′-^{32}P-labeled D-1 or M-1 (100 nM) in buffer A () were pre-equilibrated before Mg^{2+} (15 mM) was added to initiate the exonuclease reaction. The molar amount of remaining substrate was plotted as a function of time (Figure 5), and the data were fit to eq 4 () to

Table 6: Comparison of the Base Substitution Fidelity of PolB1 exo- and Four Other DNA Polymerases and HIV-1 Reverse Transcriptase

polymerase	polymerase family	F_{pol}[a]	affinity difference $[(K_d)_{incorrect}/(K_d)_{correct}]$	rate difference $[(k_p)_{correct}/(k_p)_{incorrect}]$
PolB1 exo-[b]	B	3.5×10^{-6} to 1.2×10^{-4}	109 to 918	4 to 589
Dpo4[c]	Y	1.5×10^{-4} to 3.2×10^{-3}	1 to 18	2.4×10^{2} to 1.7×10^{3}
rPolβ[d]	X	1.1×10^{-5} to 5.9×10^{-4}	35 to 342	28 to 708
hPolγ[e]	A	4.6×10^{-7} to 2.9×10^{-4}	42 to 900	39 to 1.2×10^{4}
T7 DNA Pol[f]	A	2.6×10^{-7} to 6.7×10^{-6}	200 to 400	2.0×10^{3} to 4.0×10^{3}
HIV-1 RT[g]	RT	5.9×10^{-5} to 5.8×10^{-4}	210 to 310	7 to 80

[a] Calculated as $(k_p/K_d)_{incorrect}/[(k_p/K_d)_{correct} + (k_p/K_d)_{incorrect}]$. [b] At 37 °C (this work). [c] At 37 °C (*26*). [d] At 37 °C (*36*). [e] At 37 °C, excluding the fidelity contribution from the 3′ → 5′ exonuclease activity (*10*). [f] At 20 °C, excluding the fidelity contribution from the 3′ → 5′ exonuclease activity (*9*). [g] At 37 °C and with a DNA substrate (*35*).

yield k_{exo} and reaction amplitudes (A). The k_{exo} and A values are 0.44 ± 0.02 s^{-1} and 91 nM for matched D-1 DNA and 1.86 ± 0.08 s^{-1} and 94 nM for mismatched M-1 DNA, respectively. Thus, at the primer−template junction, a mismatched dA·dA base pair was excised with a 3-fold faster rate than a matched base pair, dA·dT.

DISCUSSION

Pre-steady-state kinetic methods have been used to determine the fidelity of several DNA polymerases and to establish a kinetic basis for the fidelity of each of them (*3*, *9*−*12*, *26*, *32*, *33*, *35*−*39*). By employing these methods, we first measured the base substitution fidelity of the exonuclease-deficient PolB1 from *S. solfataricus* P2 at 37 °C. The kinetic parameters for all 16 possible single-nucleotide incorporations under single-turnover reaction conditions were individually determined. The base substitution fidelity (F_{pol}) of PolB1 exo- was determined to be in the range of 10^{-4} to 10^{-6} (Table 2). Additionally, PolB1 incorporated four correct incorporations with 6−60-fold higher substrate specificity than Dpo4 (*26*), a DNA lesion bypass Y-family polymerase from the same archaeon *S. solfataricus* P2. Both the high substrate specificity for correct incorporations and the low incorporation efficiency for misincorporations contributed to the F_{pol} of PolB1 exo-. Because the average k_p/K_d for four correct incorporations (1.3 μM^{-1} s^{-1}) was 6800-fold higher than the average k_p/K_d for 12 misincorporations (1.9×10^{-4} μM^{-1} s^{-1}), the calculation formula of F_{pol} can be rearranged as shown below:

$$\begin{aligned} F_{pol} &= (k_p/K_d)_{incorrect}/[(k_p/K_d)_{correct} \\ &\quad + (k_p/K_d)_{incorrect}] \approx (k_p/K_d)_{incorrect}/(k_p/K_d)_{correct} \\ &= [(K_d)_{incorrect}/(K_d)_{correct}]^{-1}[(k_p)_{correct}/(k_p)_{incorrect}]^{-1} \\ &= (\text{affinity difference})^{-1}(\text{rate difference})^{-1} \end{aligned} \quad (5)$$

In eq 5, F_{pol} is approximately equal to the ratio of substrate specificities of correct and incorrect nucleotides and is inversely proportional to both the apparent affinity difference [defined as $(K_d)_{incorrect}/(K_d)_{correct}$] and to the rate difference [defined as $(k_p)_{correct}/(k_p)_{incorrect}$]. For correct incorporations, the K_d values were in the range of 4−11 μM while the k_p values were in the range of 5−12 s^{-1} (Table 2). In comparison, the measurable apparent K_d values were in the range of 900−4500 μM while the measurable k_p values were in the range of 0.009−1.7 s^{-1} for incorrect incorporations (Table 2). For each D-DNA substrate (Table 1), we then calculated the apparent affinity difference and the rate difference which provided 109−918- and 4−589-fold contributions, respectively, to the F_{pol} of PolB1 exo- (Table 6). Interestingly, the apparent affinity difference was much larger than that observed with Dpo4 (*26*) but similar to those observed with the exonuclease-deficient T7 DNA polymerase (T7 DNA Pol) (*9*), human mitochondrial DNA polymerase γ (hPolγ) (*10*), rat DNA polymerase β (rPolβ) (*36*), and human immunodeficiency virus type 1 reverse transcriptase (HIV-1 RT) (*35*) (Table 6). The selection provided by nucleotide ground-state binding affinity reflects the tightness of a replicative polymerase's active site and the strength of the interactions between active site residues and an incoming nucleotide (*26*). For example, Dpo4, a low-fidelity Y-family enzyme which binds both correct and incorrect nucleotides weakly (*26*), possesses a loose active site which interacts minimally with an incoming nucleotide (*22*). Conversely, more intimate contacts between the enzyme and dNTP have been observed in the ternary crystal structures (E·DNA·dNTP) of high-fidelity DNA polymerases (*40*−*44*) and HIV-1 RT (*45*), which possess tighter active sites than the Y-family DNA polymerases. A tight polymerase active site can select a correct versus incorrect nascent base pair by shape, leading to high base selectivity (*46*). Therefore, we hypothesize that the active site of PolB1 is relatively tight and interacts extensively with an incoming nucleotide. Thermodynamically, this hypothesis is reasonable since the average apparent affinity difference (374) with PolB1 corresponds to a $\Delta\Delta G$ $\{= RT \ln[(K_d)_{incorrect}/(K_d)_{correct}]\}$ of 3.8 kcal/mol. This value is larger than the free energy differences (0.3−1.0 kcal/mol at 37 °C) between correct and incorrect base pairs at the primer terminus measured through DNA melting experiments (*47*). Thus, the differential interactions between correct and incorrect nucleotides with the polymerase active site residues of PolB1 provided a free energy difference of 2.6−3.3 kcal/mol for nucleotide selection. To further evaluate our above hypothesis, we are currently attempting to determine the ternary crystal structure of PolB1 (PolB1·DNA·dNTP). Interestingly, Table 6 also shows that the rate difference, although varying in a large range, does contribute to the F_{pol} of all five DNA polymerases from four different families. This suggests that the nucleotide incorporation step provides a common and important fidelity checkpoint during polymerization (*48*). Thus, the polymerase activity of PolB1 uses both the nucleotide binding step and the nucleotide incorporation step to discriminate against incorrect nucleotides (Table 6).

Cost of Proofreading. During proofreading, the 3′ → 5′ exonuclease activity selectively excises mismatched bases on a primer's 3′-terminus. Although rare, this activity can also cleave matched bases and slow DNA synthesis. The "cost" of utilizing this editing function has been previously defined as the ratio of the excision rate of matched DNA (k_{exo}) to the incorporation rate

of the next correct nucleotide (k_p) (*4*). PolB1 excised matched D-1 (Table 1) at a rate of 0.44 s^{-1} (Figure 5), while its polymerase domain incorporated correct dTTP into D-1 at a rate of 8.2 s^{-1} (Table 2). Thus, the cost of proofreading at 37 °C is calculated to be 5.4% which is 38-fold higher than the value of 0.14% observed with the human mitochondrial DNA polymerase complex (*4*). Such costly proofreading activity could be caused by either nonphysiological reaction conditions (e.g., temperature and pH) or the absence of a potential accessory protein to PolB1 (see below). These possibilities are being investigated in our laboratory.

Contribution of the 3′→5′ Exonuclease Activity to the Fidelity of PolB1 at 37 °C. When the polymerase activity of PolB1 incorporates an incorrect nucleotide under single-turnover conditions, one of the following competing pathways will occur if the DNA substrate does not dissociate from PolB1: the misincorporated nucleotide will be excised with a rate of k_{exo} by the 3′ → 5′ exonuclease activity, or polymerization will proceed with a rate of k_p to bury the misincorporated nucleotide by a correct nucleotide. On the basis of the kinetic partitioning between these two pathways, we define the mismatch removal probability as the ratio of $k_{exo}/(k_{exo}+k_p)$ and the mismatch extension probability as the ratio of $k_p/(k_{exo}+k_p)$. If the first pathway dominates, then the mismatch removal probability and the mismatch extension probability will approach 100 and 0%, respectively. Therefore, the 3′→5′ exonuclease activity will significantly increase the polymerization fidelity of PolB1. Thus, we further define the component (F_{exo}) contributed by the 3′→5′ exonuclease to the overall fidelity of PolB1 as

$$F_{exo} = \text{mismatch removal probability/mismatch extension probability} = k_{exo}/k_p$$

For M-1 (Table 1), the single mismatched dA·dA base pair at the junction of the primer and template was excised with a k_{exo} of 1.86 s^{-1} (Figure 5) while it was extended by a correct dCTP with a k_p of 0.13 s^{-1} (Table 5), resulting in a removal probability of 93%, a mismatch extension probability of 7%, and an F_{exo} of 14. Because the mismatch extension fidelity (Table 5) was high, we did not consider the possibility of misincorporations during mismatch extension. Considering that F_{pol} is in the range of 10^{-4} to 10^{-6} (Table 2), the overall fidelity of PolB1, which is the ratio of F_{pol} and F_{exo}, was calculated to be in the range of 10^{-5} to 10^{-7}. In addition to reaction conditions (pH and temperature), this fidelity can be affected by the following factors: (i) faster intramolecular transfer of mismatched than matched DNA from the polymerase to the exonuclease active site, (ii) mismatched DNA dissociates faster than matched DNA from the polymerase active site, and (iii) mismatched DNA binds faster than matched DNA to the 3′ → 5′ exonuclease active site. These factors have been proven to contribute to the fidelity of T7 DNA Pol (*3*, *9*) and hPolγ (*4*) in which the 3′ → 5′ exonuclease activity enhances their overall fidelity by ~200-fold. We are currently investigating the potential contributions of these factors to the overall fidelity of PolB1. Moreover, the enzymatic properties, including fidelity of several replicative DNA polymerases, have been found to be altered by their accessory proteins. For example, the fidelity of hPolγ is increased by 14-fold with its accessory subunit (*12*). With regard to PolB1, a similar accessory protein has not been identified, although the genome of *S. solfataricus* P2 encodes a heterotrimer of proliferating cell nuclear antigen.

Insignificant Effect of Temperature on the Base Substitution Fidelity of the Polymerase Activity of PolB1. When the reaction temperature increased from 19 to 50 °C, Table 3 shows that the base substitution fidelity of PolB1 exo- decreased by only 5-fold. A similar modest increase in base substitution rates with temperature has been observed with *S. solfataricus* Dpo4 (*25*, *33*), the exonuclease-deficient *Thermus aquaticus* (*Taq*) DNA polymerase (*14*), *Vent* DNA polymerase (*15*), and T4 DNA polymerase (*13*, *16*). Therefore, we project the base substitution fidelity of PolB1 exo- in vivo (80 °C) will be slightly higher than the fidelity value calculated at 50 °C (Table 3). As in our previous kinetic analysis of the temperature effect on the fidelity of Dpo4 (*33*), the kinetic basis for the small decrease in the base substitution fidelity of PolB1 exo- was due to a similar change in magnitude of the k_p/K_d with temperature for both correct and incorrect dNTP incorporations (Table 3). Also similar to Dpo4 (*33*), the apparent ground-state binding affinities of both correct and incorrect nucleotides and their ratio $(K_d)_{incorrect}/(K_d)_{correct}$ were altered slightly over a temperature range of 31 °C. In stark contrast, PolB1 exo- catalyzed the incorporations of both correct and incorrect nucleotides with a much faster k_p at 50 °C than at 19 °C. This indicated that PolB1, like Dpo4 (*33*), becomes more dynamic at higher temperatures. The contribution of increased protein dynamics of PolB1 to catalysis is discussed in detail in the accompanying paper (*31*).

Higher Polymerization Fidelity of PolB1 at Lower pH. Using M13mp2-based fidelity assays, the base substitution fidelity of several DNA polymerases, including the exonuclease-deficient *Taq* DNA polymerase (*49*) and *E. coli* DNA polymerase I (*50*), has been found to be ~10−60-fold higher when the reaction pH is lowered by three units from pH 8−9 to 5−6 (*49*−*51*). Consistently, the base substitution fidelity of PolB1 exo- increased by 36-fold when the reaction pH was decreased from 8.5 to 6.0 (Table 4). Thus, both kinetic and M13mp2-based fidelity assays indicate that these DNA polymerases are less faithful at higher pH. Mechanistically, the 36-fold drop in the polymerase fidelity of PolB1 exo- when the reaction pH was increased from 6.0 to 8.5 was contributed by both a 10-fold lower incorporation efficiency of correct dTTP and a 3.6-fold higher k_p/K_d for incorrect dATP incorporation (Table 4). Moreover, these changes in the incorporation efficiency were due mostly to a 7-fold increase in the apparent K_d for correct dTTP incorporation and a 10-fold increase in the k_p for dATP misincorporation. Interestingly, the cytoplasmic pH of another *Sulfolobus* species, *Sulfolobus acidocaldarius*, has been estimated to be ~6.0 (*52*), although this organism grows optimally under harsh environmental conditions (80 °C and pH 2−4) like *S. solfataricus* (*18*). On the basis of the physiological similarity between these two *Sulfolobus* species, we hypothesize that the cytoplasmic pH of *S. solfataricus*, which has not been measured, is approximately 6.0. At this pH, the polymerase activity of PolB1 will have a base substitution fidelity 25-fold higher than the fidelity at pH 7.5 (Table 2). After offsetting the opposing effects of temperature and pH on the F_{pol}, we further estimate the overall fidelity of PolB1 to be in the range of 10^{-6} to 10^{-8} in vivo.

Biological Relevance of the Kinetically Estimated Fidelity of PolB1. Although inhabiting environments at extremely high temperature and low pH, hyperthermophilic archaea have much lower genetic mutation rates than other DNA microbes and eukaryotes (*53*). For example, the base substitution frequency of *S. acidocaldarius* when it is growing at pH 3.5 and 75 °C is 3.2×10^{-10} per base (*53*). Although such a frequency for *S. solfataricus* has not been reported, we estimated it to be either 3.2×10^{-10} or 100-fold higher on the basis of the following in vivo

observation: the average frequency of spontaneous mutations in *S. solfataricus*, which are dominated by transposon mutagenesis, is at least 50−60-fold higher than the one in *S. acidocaldarius* (*54*). Taken together, we estimate the base substitution frequency in *S. solfataricus* to be in the range of 10^{-8} to 10^{-10} per base. This frequency is ~100-fold lower than the estimated error rate (10^{-6} to 10^{-8}) of PolB1 in vitro (see the above discussion). Although the effects of several kinetic factors and a potential accessory protein may further decrease the error rate of PolB1, other cellular proteins or pathways clearly play a major role in lowering the substitution frequency in *S. solfataricus*. For example, active DNA repair pathways have been proposed to maintain the overall genetic fidelity in *S. acidocaldarius* (*53*). Similar pathways in *S. solfataricus* likely correct most misincorporations generated by PolB1 or other polymerases in vivo.

SUPPORTING INFORMATION AVAILABLE

Comparison of polymerase and 3′ → 5′ exonuclease activity for PolB1 enzymes (Figure 1). This material is available free of charge via the Internet at http://pubs.acs.org.

REFERENCES

1. Hubscher, U., Maga, G., and Spadari, S. (2002) Eukaryotic DNA polymerases. *Annu. Rev. Biochem. 71*, 133–163.
2. Fowler, J. D., and Suo, Z. (2006) Biochemical, structural, and physiological characterization of terminal deoxynucleotidyl transferase. *Chem. Rev. 106*, 2092–2110.
3. Donlin, M. J., Patel, S. S., and Johnson, K. A. (1991) Kinetic partitioning between the exonuclease and polymerase sites in DNA error correction. *Biochemistry 30*, 538–546.
4. Johnson, A. A., and Johnson, K. A. (2001) Exonuclease proofreading by human mitochondrial DNA polymerase. *J. Biol. Chem. 276*, 38097–38107.
5. Kuchta, R. D., Benkovic, P., and Benkovic, S. J. (1988) Kinetic mechanism whereby DNA polymerase I (Klenow) replicates DNA with high fidelity. *Biochemistry 27*, 6716–6725.
6. Capson, T. L., Peliska, J. A., Kaboord, B. F., Frey, M. W., Lively, C., Dahlberg, M., and Benkovic, S. J. (1992) Kinetic characterization of the polymerase and exonuclease activities of the gene 43 protein of bacteriophage T4. *Biochemistry 31*, 10984–10994.
7. Kuchta, R. D., Mizrahi, V., Benkovic, P. A., Johnson, K. A., and Benkovic, S. J. (1987) Kinetic mechanism of DNA polymerase I (Klenow). *Biochemistry 26*, 8410–8417.
8. Patel, S. S., Wong, I., and Johnson, K. A. (1991) Pre-steady-state kinetic analysis of processive DNA replication including complete characterization of an exonuclease-deficient mutant. *Biochemistry 30*, 511–525.
9. Wong, I., Patel, S. S., and Johnson, K. A. (1991) An induced-fit kinetic mechanism for DNA replication fidelity: Direct measurement by single-turnover kinetics. *Biochemistry 30*, 526–537.
10. Lee, H. R., and Johnson, K. A. (2006) Fidelity of the human mitochondrial DNA polymerase. *J. Biol. Chem. 281*, 36236–36240.
11. Zhang, H., Rhee, C., Bebenek, A., Drake, J. W., Wang, J., and Konigsberg, W. (2006) The L561A substitution in the nascent base-pair binding pocket of RB69 DNA polymerase reduces base discrimination. *Biochemistry 45*, 2211–2220.
12. Johnson, A. A., and Johnson, K. A. (2001) Fidelity of nucleotide incorporation by human mitochondrial DNA polymerase. *J. Biol. Chem. 276*, 38090–38096.
13. Bessman, M. J., and Reha-Krantz, L. J. (1977) Studies on the biochemical basis of spontaneous mutation. V. Effect of temperature on mutation frequency. *J. Mol. Biol. 116*, 115–123.
14. Tindall, K. R., and Kunkel, T. A. (1988) Fidelity of DNA synthesis by the *Thermus aquaticus* DNA polymerase. *Biochemistry 27*, 6008–6013.
15. Mattila, P., Korpela, J., Tenkanen, T., and Pitkanen, K. (1991) Fidelity of DNA synthesis by the *Thermococcus litoralis* DNA polymerase: An extremely heat stable enzyme with proofreading activity. *Nucleic Acids Res. 19*, 4967–4973.
16. Smith, L. A., and Drake, J. W. (1998) Aspects of the ultraviolet photobiology of some T-even bacteriophages. *Genetics 148*, 1611–1618.
17. Kunkel, T. A. (2004) DNA replication fidelity. *J. Biol. Chem. 279*, 16895–16898.
18. She, Q., Singh, R. K., Confalonieri, F., Zivanovic, Y., Allard, G., Awayez, M. J., Chan-Weiher, C. C., Clausen, I. G., Curtis, B. A., De Moors, A., Erauso, G., Fletcher, C., Gordon, P. M., Heikamp-de Jong, I., Jeffries, A. C., Kozera, C. J., Medina, N., Peng, X., Thi-Ngoc, H. P., Redder, P., Schenk, M. E., Theriault, C., Tolstrup, N., Charlebois, R. L., Doolittle, W. F., Duguet, M., Gaasterland, T., Garrett, R. A., Ragan, M. A., Sensen, C. W., and Van der Oost, J. (2001) The complete genome of the crenarchaeon Sulfolobus solfataricus P2. *Proc. Natl. Acad. Sci. U.S.A. 98*, 7835–7840.
19. Prangishvili, D., and Klenk, H. P. (1993) Nucleotide sequence of the gene for a 74 kDa DNA polymerase from the archaeon *Sulfolobus solfataricus*. *Nucleic Acids Res. 21*, 2768.
20. Edgell, D. R., Klenk, H. P., and Doolittle, W. F. (1997) Gene duplications in evolution of archaeal family B DNA polymerases. *J. Bacteriol. 179*, 2632–2640
21. Boudsocq, F., Iwai, S., Hanaoka, F., and Woodgate, R. (2001) *Sulfolobus solfataricus* P2 DNA polymerase IV (Dpo4): An archaeal DinB-like DNA polymerase with lesion-bypass properties akin to eukaryotic poleta. *Nucleic Acids Res. 29*, 4607–4616
22. Ling, H., Boudsocq, F., Woodgate, R., and Yang, W. (2001) Crystal structure of a Y-family DNA polymerase in action: A mechanism for error-prone and lesion-bypass replication. *Cell 107*, 91–102
23. Ling, H., Sayer, J. M., Plosky, B. S., Yagi, H., Boudsocq, F., Woodgate, R., Jerina, D. M., and Yang, W. (2004) Crystal structure of a benzo[a]pyrene diol epoxide adduct in a ternary complex with a DNA polymerase. *Proc. Natl. Acad. Sci. U.S.A. 101*, 2265–2269
24. Mizukami, S., Kim, T. W., Helquist, S. A., and Kool, E. T. (2006) Varying DNA base-pair size in subangstrom increments: Evidence for a loose, not large, active site in low-fidelity Dpo4 polymerase. *Biochemistry 45*, 2772–2778
25. Kokoska, R. J., Bebenek, K., Boudsocq, F., Woodgate, R., and Kunkel, T. A. (2002) Low fidelity DNA synthesis by a y family DNA polymerase due to misalignment in the active site. *J. Biol. Chem. 277*, 19633–19638
26. Fiala, K. A., and Suo, Z. (2004) Pre-Steady-State Kinetic Studies of the Fidelity of *Sulfolobus solfataricus* P2 DNA Polymerase IV. *Biochemistry 43*, 2106–2115
27. Pisani, F. M., De Martino, C., and Rossi, M. (1992) A DNA polymerase from the archaeon *Sulfolobus solfataricus* shows sequence similarity to family B DNA polymerases. *Nucleic Acids Res. 20*, 2711–2716
28. Pisani, F. M., Manco, G., Carratore, V., and Rossi, M. (1996) Domain organization and DNA-induced conformational changes of an archaeal family B DNA polymerase. *Biochemistry 35*, 9158–9166
29. Lou, H., Duan, Z., Sun, T., and Huang, L. (2004) Cleavage of double-stranded DNA by the intrinsic 3′-5′ exonuclease activity of DNA polymerase B1 from the hyperthermophilic archaeon *Sulfolobus solfataricus* at high temperature. *FEMS Microbiol. Lett. 231*, 111–117
30. Savino, C., Federici, L., Johnson, K. A., Vallone, B., Nastopoulos, V., Rossi, M., Pisani, F. M., and Tsernoglou, D. (2004) Insights into DNA replication: the crystal structure of DNA polymerase B1 from the archaeon *Sulfolobus solfataricus*. *Structure 12*, 2001–2008
31. Brown, J. A., and Suo, Z. (2009) Elucidating the kinetic mechanism of DNA polymerization catalyzed by *Sulfolobus solfataricus* P2 DNA polymerase B1. *Biochemistry* (DOI 10.1021/bi9005336)
32. Fiala, K. A., and Suo, Z. (2004) Mechanism of DNA Polymerization Catalyzed by *Sulfolobus solfataricus* P2 DNA Polymerase IV. *Biochemistry 43*, 2116–2125
33. Fiala, K. A., Sherrer, S. M., Brown, J. A., and Suo, Z. (2008) Mechanistic consequences of temperature on DNA polymerization catalyzed by a Y-family DNA polymerase. *Nucleic Acids Res. 36*, 1990–2001
34. Tsai, Y. C., and Johnson, K. A. (2006) A new paradigm for DNA polymerase specificity. *Biochemistry 45*, 9675–9687
35. Kati, W. M., Johnson, K. A., Jerva, L. F., and Anderson, K. S. (1992) Mechanism and fidelity of HIV reverse transcriptase. *J. Biol. Chem. 267*, 25988–25997
36. Ahn, J., Kraynov, V. S., Zhong, X., Werneburg, B. G., and Tsai, M. D. (1998) DNA polymerase β: Effects of gapped DNA substrates on dNTP specificity, fidelity, processivity and conformational changes. *Biochem. J. 331* (Part 1), 79–87
37. Washington, M. T., Prakash, L., and Prakash, S. (2001) Yeast DNA polymerase η utilizes an induced-fit mechanism of nucleotide incorporation. *Cell 107*, 917–927

38. Roettger, M. P., Fiala, K. A., Sompalli, S., Dong, Y., and Suo, Z. (2004) Pre-steady-state kinetic studies of the fidelity of human DNA polymerase μ. *Biochemistry 43*, 13827–13838
39. Fiala, K. A., Duym, W. W., Zhang, J., and Suo, Z. (2006) Up-regulation of the fidelity of human DNA polymerase λ by its non-enzymatic proline-rich domain. *J. Biol. Chem. 281*, 19038–19044.
40. Eom, S. H., Wang, J., and Steitz, T. A. (1996) Structure of Taq polymerase with DNA at the polymerase active site. *Nature 382*, 278–281.
41. Sawaya, M. R., Prasad, R., Wilson, S. H., Kraut, J., and Pelletier, H. (1997) Crystal structures of human DNA polymerase β complexed with gapped and nicked DNA: Evidence for an induced fit mechanism. *Biochemistry 36*, 11205–11215.
42. Wang, J., Sattar, A. K., Wang, C. C., Karam, J. D., Konigsberg, W. H., and Steitz, T. A. (1997) Crystal structure of a pol α family replication DNA polymerase from bacteriophage RB69. *Cell 89*, 1087–1099.
43. Doublie, S., Tabor, S., Long, A. M., Richardson, C. C., and Ellenberger, T. (1998) Crystal structure of a bacteriophage T7 DNA replication complex at 2.2 Å resolution. *Nature 391*, 251–258.
44. Li, Y., Korolev, S., and Waksman, G. (1998) Crystal structures of open and closed forms of binary and ternary complexes of the large fragment of *Thermus aquaticus* DNA polymerase I: Structural basis for nucleotide incorporation. *EMBO J. 17*, 7514–7525.
45. Huang, H., Chopra, R., Verdine, G. L., and Harrison, S. C. (1998) Structure of a covalently trapped catalytic complex of HIV-1 reverse transcriptase: Implications for drug resistance. *Science 282*, 1669–1675.
46. Kool, E. T. (2002) Active site tightness and substrate fit in DNA replication. *Annu. Rev. Biochem. 71*, 191–219.
47. Petruska, J., Goodman, M. F., Boosalis, M. S., Sowers, L. C., Cheong, C., and Tinoco, I.Jr. (1988) Comparison between DNA melting thermodynamics and DNA polymerase fidelity. *Proc. Natl. Acad. Sci. U.S.A. 85*, 6252–6256.
48. Joyce, C. M., and Benkovic, S. J. (2004) DNA polymerase fidelity: Kinetics, structure, and checkpoints. *Biochemistry 43*, 14317–14324.
49. Eckert, K. A., and Kunkel, T. A. (1990) High fidelity DNA synthesis by the *Thermus aquaticus* DNA polymerase. *Nucleic Acids Res. 18*, 3739–3744.
50. Eckert, K. A., and Kunkel, T. A. (1993) Effect of reaction pH on the fidelity and processivity of exonuclease-deficient Klenow polymerase. *J. Biol. Chem. 268*, 13462–13471.
51. Eckert, K. A., and Kunkel, T. A. (1993) Fidelity of DNA synthesis catalyzed by human DNA polymerase α and HIV-1 reverse transcriptase: Effect of reaction pH. *Nucleic Acids Res. 21*, 5212–5220.
52. Meyer, W., and Schafer, G. (1992) Characterization and purification of a membrane-bound archaebacterial pyrophosphatase from *Sulfolobus acidocaldarius*. *Eur. J. Biochem. 207*, 741–746.
53. Grogan, D. W., Carver, G. T., and Drake, J. W. (2001) Genetic fidelity under harsh conditions: Analysis of spontaneous mutation in the thermoacidophilic archaeon *Sulfolobus acidocaldarius*. *Proc. Natl. Acad. Sci. U.S.A. 98*, 7928–7933.
54. Martusewitsch, E., Sensen, C. W., and Schleper, C. (2000) High spontaneous mutation rate in the hyperthermophilic archaeon *Sulfolobus solfataricus* is mediated by transposable elements. *J. Bacteriol. 182*, 2574–2581.